

Threading dislocation reduction in strained layers

A. E. Romanov

A. F. Ioffe Physico-Technical Institute, 194021 St. Petersburg, Russia

W. Pompe

Technical University, Hallwachsstrasse 3, 01069 Dresden, Germany

S. Mathis

Materials Department, University of California, Santa Barbara, California 93106

G. E. Beltz

Mechanical Engineering Department, University of California, Santa Barbara, California 93106

J. S. Speck^{a)}

Materials Department, University of California, Santa Barbara, California 93106

(Received 8 May 1998; accepted for publication 29 September 1998)

In this article, we have developed models for threading dislocation (TD) reduction due to the introduction of an intentionally strained layer. Three different types of dislocations have been considered in this model: misfit dislocations (MDs), mobile TDs, and TDs whose glide motion has been blocked by a MD crossing the glide path of the TD (immobile TDs). The models are based on MD formation by the process of lateral TD motion. The strain-induced TD motion leads to possible annihilation reactions of mobile TDs with either other mobile TDs or blocked TDs, or reactions in which a mobile TD is converted to an immobile TD by a blocking reaction with a MD. The evolution of the density of mobile and blocked TDs and the MD density is represented by three coupled nonlinear first order differential equations. When blocking of TDs by MDs is not considered, the equations have an analytical solution that shows that the final TD density should decrease exponentially where the argument of the exponent is proportional to the product of the reaction radius between TDs (the annihilation radius r_A) and the nominal misfit strain ϵ_m . The no-blocking limit represents the maximum possible TD reduction through the introduction of a strained layer, regardless whether this layer has a discrete step in strain, step-grade, or continuous strain grading. When only blocking reactions are considered (no annihilation), again analytic solutions to the equations are obtained which show the maximum possible plastic strain relaxation for a discretely strained layer. Several examples of numerical solutions to the three coupled differential equations are described for cases that include both blocking and annihilation reactions.

© 1999 American Institute of Physics. [S0021-8979(99)04901-4]

I. INTRODUCTION

During the past 25 years a large body of research has been established on the theory and experiments for strain relaxation by misfit dislocations (MDs) for lattice mismatched epitaxial films (see, for example, the articles by Beanland *et al.*,¹ Freund,² and Fitzgerald³). In the growth of lattice-mismatched epitaxial thin films, threading dislocations (TDs) are concomitantly generated with MDs. For a wide variety of electronic and optoelectronic device applications, particularly for minority carrier devices, TDs are deleterious for physical performance. In recent years there has been a substantial experimental effort to reduce TD densities. Despite the great amount of literature devoted to theoretical and experimental understanding of critical thicknesses for MD generation, there have been relatively few theoretical efforts reported to understand the mechanisms by which TDs are eliminated in thin films.

In previous work on TD reduction in mismatched layers, it was shown that in laterally uniform layers, the TD density can only be reduced through reaction with other TDs.^{4,5} The two reduction reactions are annihilation, in which TDs with opposite Burgers vectors meet, or fusion, in which two TDs react to form a single TD.⁴⁻⁸ Relative motion between TDs is necessary to bring them within a reaction distance. It was shown that the possible sources of motion include “trajectory” motion of the TDs with changing film thickness, which is due to different TDs having different line directions (because of their Burgers vectors and slip planes). Motion may also be induced by condensation of point defects at a TD, leading to either positive climb (vacancy condensation) or negative climb (interstitial condensation).^{5,9} Finally, TD motion may be induced by intentional growth of a strained layer. In this case, when the film excess a critical thickness h_c , misfit dislocation generation accompanies the glide motion of TDs.

The reactions among TDs can be analytically modeled using a “reaction kinetics” approach.⁴⁻⁷ In this method, the change in TD density with an evolutionary variable, usually

^{a)}Electronic mail: speck@mr1.ucsb.edu

film thickness, can be represented by a first order differential equation. In the simplest case, only the total TD density was considered. In a more involved approach, a series of coupled ordinary first order nonlinear differential equations was formulated. Each equation represents the change in the density of a particular character TD (determined by its Burgers vector, line direction, and slip plane). Since two TDs must react to reduce the TD density, each equation in the series of equations is a sum of terms in which the individual terms are the products of specific TD densities with a coefficient based on geometry and interaction strength between the specific character TDs. In relation to chemical kinetics, the film thickness evolution is analogous to time and the specific TD densities are analogous to chemical reactant concentrations. The interaction constant for TD reactions, analogous to a rate constant in chemical kinetics, is referred to as either the annihilation radius r_A or the fusion radius r_F . These two interaction constants represent the distance necessary for spontaneous reaction between the TDs. Using this approach, with the full details of the TD geometry in (001) face-centered cubic (fcc) semiconductor heteroepitaxy, the experimentally observed behavior of the total TD density (inversely proportional to the film thickness) was reproduced in the solutions for the total TD density. Additionally, the solutions for the coupled differential equations showed a saturation in TD density when the initial TD density had a net Burgers vector content.

The experimental observation and theoretical prediction that the TD density in relaxed buffer layers will be inversely proportional to the buffer layer thickness h motivates other approaches for efficiently reducing TD densities because low TD densities, in the range of 10^5 – 10^6 cm^{-2} , may require the use of very thick buffer layers. The use of strained layers is particularly promising as, once the strained layer exceeds its critical thickness, there can be substantial lateral motion of TDs as they generate MD segments. X-ray topography studies have shown that in the growth of strained layers on single crystal substrates the threading dislocations originating in the substrate bend to form MD segments at strained layer thicknesses very close to the Matthews–Blakeslee critical thickness.¹⁰ For growth on single crystal substrates, the TD density is generally too low (e.g., GaAs substrates can typically be obtained with TD densities on the order of 10^4 cm^{-2}) to provide a substantial MD density. Therefore, growth of thick strained layers on high quality single crystal substrates will lead to the generation of a high density of TDs during strain relaxation.

In this article we model the TD reduction during the growth of strained layers within the framework of the “kinetic approach.” The underlying layer for these models, referred to as the substrate, is strain relaxed and has a high TD density (e.g., in the range 10^6 – 10^{11} cm^{-2}) which is associated with misfit relaxation processes with a further underlying layer. In the models developed here, we treat the concurrent TD reduction through annihilation reactions that result from TD–TD reactions during strain-driven TD motion. Additionally, we analytically treat the blocking of mobile TDs by MDs. However, we do not include any processes that generate new TDs. In this article, we will not attempt to fit or explain the wide range of experimental data on different

strained layer approaches for reducing TD density; that is a topic for a future article.

II. BACKGROUND

The concept and validity of the Matthews–Blakeslee (MB) critical thickness for forming MDs in strained epitaxial layers has been extensively explored during the past 25 years. We follow the recent treatment of the critical thickness concept developed by Freund.² In this approach, the energetically favorable motion of a TD connected to a MD was evaluated as a function of misfit strain ϵ_m and film thickness h , as shown in Fig. 1. The critical thickness h_c is that for which the equilibrium MD density is zero; for thicknesses larger than h_c , it is energetically favorable for the TD to increase the MD line length, as shown in Fig. 1(b). This strain-driven motion of the TD leads to both plastic relief of the misfit strain, but it also leads to increased probability of the TD segment meeting another TD segment. The MB critical thickness is given as the solution of

$$h_c = \frac{|\mathbf{b}|}{8\pi\epsilon_m \cos \lambda} \left(\frac{1 - \nu \cos^2 \beta}{1 + \nu} \right) \ln \left(\frac{\alpha h_c}{|\mathbf{b}|} \right), \quad (1)$$

where $|\mathbf{b}|$ is the magnitude of the Burgers vector \mathbf{b} , λ is the angle between the Burgers vector and a line that lies in the film/substrate interface normal to the MD line, β is the angle between the MD line and \mathbf{b} , ν is Poisson’s ratio, and α is the core cutoff parameter. For the purposes of this article, we use a simplified approximation for the critical thickness h_c :

$$h_c \approx \frac{|\mathbf{b}|}{\epsilon_m} = \frac{b}{\epsilon_m}. \quad (2)$$

This approximation is justified because the product of all other terms in Eq. (1) are approximately constant (because of the weak thickness dependence of the logarithmic term) and have a magnitude on the order of one. We note that the asymptotic behaviors developed in this article for TD and MD densities for large film thicknesses do *not* depend on the exact value used for h_c .

During the motion of TDs to generate new MDs (for $h > h_c$), mobile TDs may have their motion blocked by MDs lying in the path of the moving TDs, as shown schematically in Fig. 1(c). The problem of TD blocking has been treated in detail by Freund and co-workers.^{11,12} In the models we will develop below, once a TD has been blocked by a crossing MD, its motion will be considered arrested for all further film growth. In future articles we will treat the role of “unblocking” of TDs on TD reduction and strain relaxation in strained layer growth.

The equilibrium linear MD density $\rho_{\text{MD}}^{\text{equil}}$ (the number of MDs per unit length at or near the film/substrate interface) for films with thicknesses larger than h_c can be calculated directly¹³ and is given as

$$\rho_{\text{MD}}^{\text{equil}} = \frac{\epsilon_m}{|\mathbf{b}| \cos \lambda} \left(1 - \frac{h_c}{h} \right), \quad \text{for } h > h_c. \quad (3)$$

Again, we use a simplifying approximation for the equilibrium MD density:

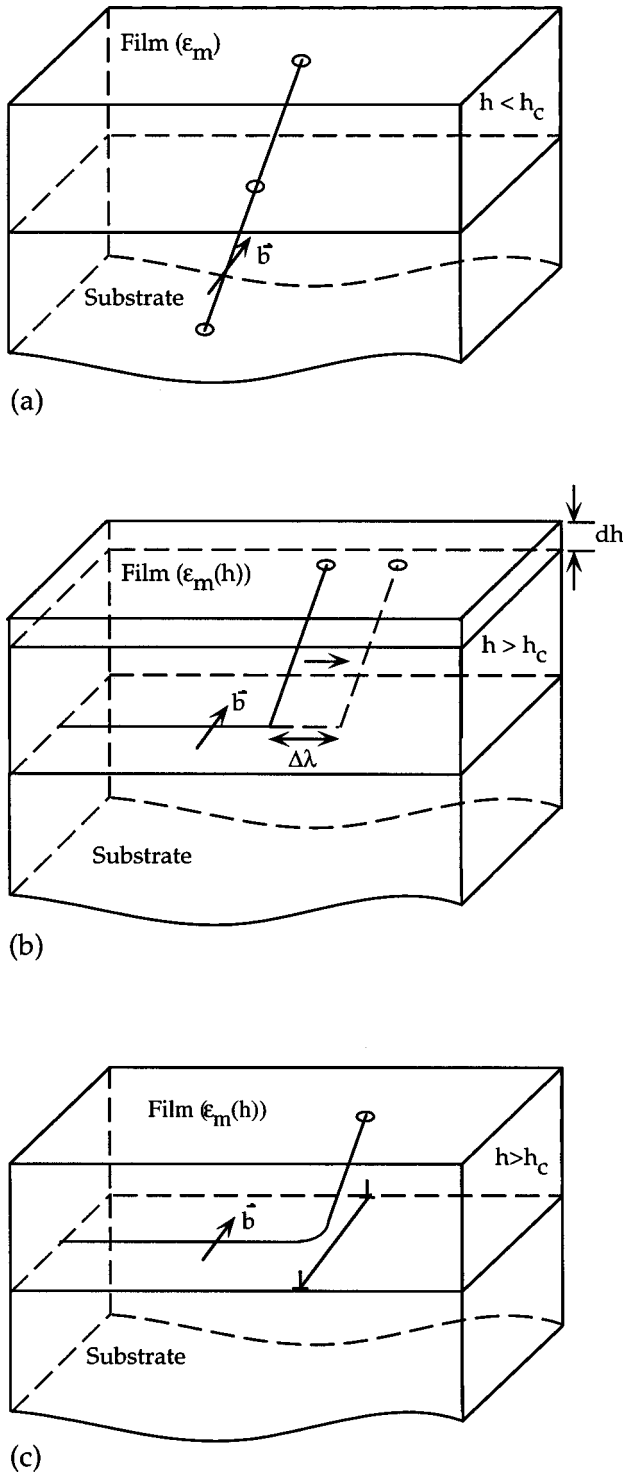


FIG. 1. Basic processes of TD motion in a strained epitaxial film. (a) An isolated TD for $h < h_c$ and thus no motion is possible. (b) TD-MD system for $h > h_c$: increasing film thickness leads to the increasing configurational force on the TD which leads to TD motion and generation of additional MD segment length. (c) Blocking of TD motion by a MD in the slip path of the TD.

$$\rho_{MD}^{equil} = \frac{1}{h_c} - \frac{1}{h}, \quad \text{for } h > h_c. \quad (4)$$

If the MD density at a thickness h is less than ρ_{MD}^{equil} , then the “excess” strain ϵ_x in the system is given as

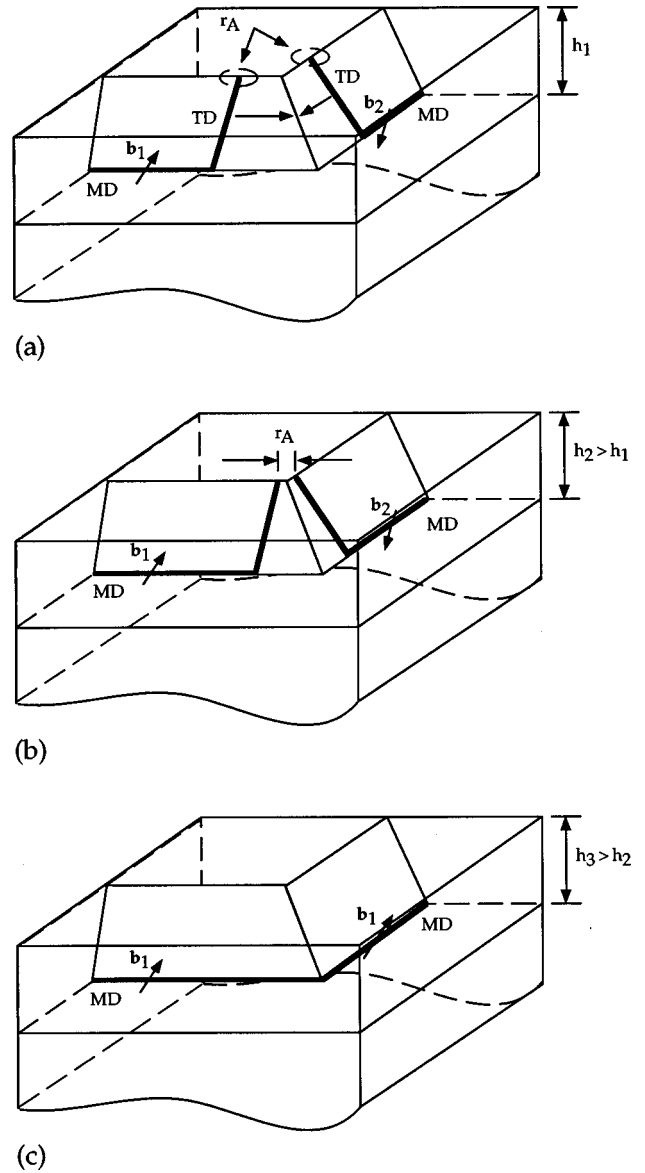


FIG. 2. Motion and annihilation of TDs in strained layers. (a) Initial configuration of two TDs with opposite Burgers vectors ($\mathbf{b}_1 = -\mathbf{b}_2$) on intersecting slip planes in a film of thickness $h_1 \leq h_c$. (b) Intermediate configuration with TDs at the distance of the annihilation radius r_A in the film with thickness $h_2 > h_1$. (c) Final configuration with MDs only (the TDs are annihilated) in the film with thickness $h_3 > h_2$.

$$\epsilon_x = \left(\frac{1}{h_c} - \frac{1}{h} - \rho_{MD} \right) b. \quad (5)$$

The critical thickness concept can now be used to illustrate misfit strain mediated TD reduction. In our previous work, we argued that the most likely process for TD reduction involved annihilation or fusion reactions between TDs lying on intersecting slip planes. Consider the example for (001) fcc epitaxy shown in Fig. 2. For this example, both the (101) and (011) slip planes have MD segments terminated by a TD. The TDs in this example have opposite Burgers vectors, $\mathbf{b}_1 = -\mathbf{b}_2$ when the outward normal sense from the film surface is used as the line direction for the TDs. For a layer with a misfit strain ϵ_m , at $h = h_1 = h_c$, the TD segments should neither move to increase nor decrease the length of

their MD segments. For $h = h_2 > h_c$, it is energetically favorable for the TDs to increase the MD segment length, as shown in Fig. 2(b). During the process of generating new MD length, the TDs may fall within an annihilation radius r_A , at which point the TDs annihilate. The product of annihilation reaction has no threading segments and the resulting MD may have a change in orientation of its line but it must have a single Burgers vector (note that for the MD segments we have changed the line direction for one of the MD segments after they fuse), as shown in Fig. 2(c). If the TD segments do not have opposite Burgers vectors, but still have an attractive force, then the two TDs will “fuse” and the resulting single TD will have a Burgers vector that is the sum of the Burgers vectors of the reacting TDs. Additionally, for fusion, the TD will form a node with the two MD segments at, or near, the film/substrate interface.

In our previous work on TD reduction in homogeneous buffer layers we considered the complete crystallography and TD geometry for (001) fcc semiconductor films.^{6,7} This treatment included all possible TDs (Burgers vector and slip plane combination). For (001) oriented films with $\frac{1}{2}\langle 110 \rangle \{111\}$ slip systems, there are 24 unique character TDs (each of the 4 inclined $\{111\}$ slip planes has six possible Burgers vectors including opposite sign). Thus, each unique TD must be described with a separate differential equation. Each TD has a 1 in 24 possibility of an annihilation reaction with other TDs and a 6 in 24 chance of a fusion reaction. When considering all possible reactions between TDs, we demonstrated that the reduction in total TD density (the sum of all 24 individual densities) with increasing film thickness (the solutions to 24 coupled differential equations) could be fit to the solution of a single differential equation for the overall dislocation density with a single coefficient K . The value of K is proportional to the annihilation radius r_A and also depends on the ratio r_F/r_A and depends on geometrical parameters. For the description of overall TD reduction, we can adjust the dependencies of K by appropriate changes to the value of r_A . In the current approach we are interested in total TD reduction due to effective annihilation reactions. Therefore in the models below we consider only annihilation reactions and treat r_A as a phenomenological parameter which describes the average overall reaction probability.

In models developed below, we assume that the threading dislocations lie on inclined slip planes such that the misfit strain directly leads to a resolved shear stress on the slip plane. Thus, the models are directly applicable, for example, to (001) epitaxy of diamond structure or zinc blende semiconductors. Note that for (0001) oriented wurzite semiconductors, the $\{hki0\}$ planes, on which the TDs normally lie, do not have a resolved shear stress for biaxial misfit or thermal stresses.

III. APPROACH

For the treatment of strained layers, we consider TDs that have no obstacles to motion, mobile TDs with density ρ_{TD}^m , and TDs whose motion is blocked by MDs. The blocked, or immobile, TDs have density ρ_{TD}^i . In all of the modeling that follows, we only consider the relaxation of an

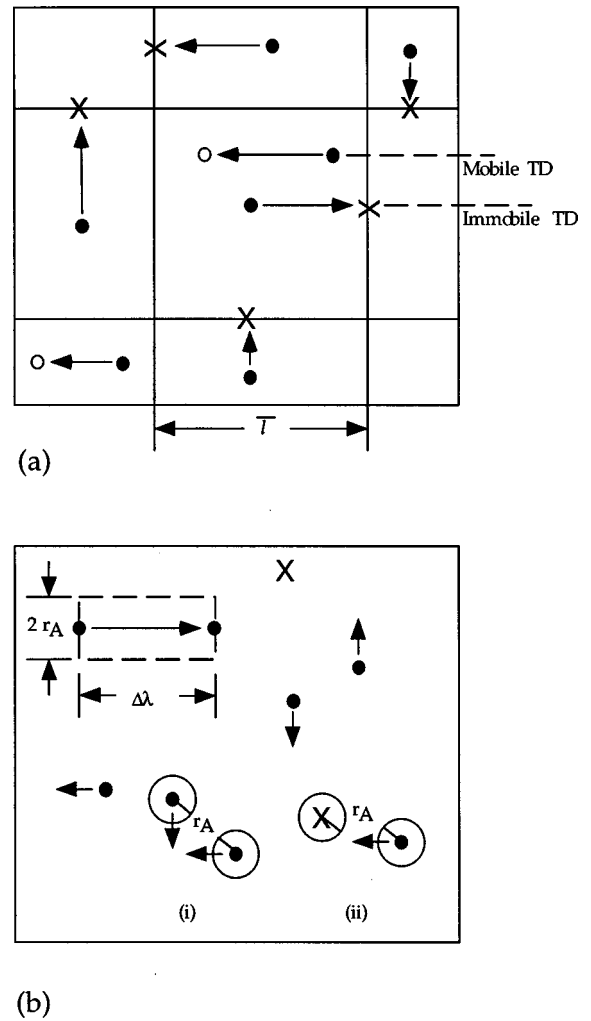


FIG. 3. Plan view schematic showing the TD geometry leading either to annihilation reactions or TD blocking due to motion of the mobile TDs. Here, a closed circle represents the initial position of a mobile TD, an open circle represents a mobile TD after motion, and a \times represents a blocked or immobile TD. (a) Blocking of mobile TDs by MDs with average spacing $\bar{l} = 1/\rho_{MD} = 1/\rho_3$. (b). Annihilation reactions: (i) between two mobile TDs; (ii) between a mobile TD and a blocked TD.

intentionally strained layer (misfit strain ϵ_m) by MD generation through the motion of mobile TDs. That is, there is no mechanism for generating new TDs (e.g., through new half-loop formation or multiplication). We initially consider the changes in TD and MD densities with differential motion $d\lambda$ of the mobile TDs. The mobile TD motion λ is driven by an intentional misfit strain, ϵ_m . We will later relate the differential motion $d\lambda$ to changes in film thickness dh . The total TD density ρ_{TD}^{total} , which is defined as the number of TDs per unit area at the film free surface, is given as

$$\rho_{TD}^{total} = \rho_{TD}^i + \rho_{TD}^m. \quad (6)$$

The changes in the TD densities ρ_{TD}^m , ρ_{TD}^i , and ρ_{MD} are all related to the motion of the mobile TDs. If we assume a cross grid of MDs, as shown schematically in Fig. 3(a), the mean spacing \bar{l} between MDs will be inversely proportional to the ρ_{MD} and for simplicity we assume there are no geometric factors in this relation, i.e., $\bar{l} = 1/\rho_{MD}$ (that is, we take the number of MD intersections with a reference line that is

perpendicular to the MD lines). The chance of intersection of a randomly located TD, with a MD line, due to TD motion $d\lambda$, is $d\lambda/l = \rho_{MD}d\lambda$ and thus $d\rho_{TD}^m = -\rho_{TD}^m\rho_{MD}d\lambda$. At such an intersection, a mobile TD, shown as an open circle in Fig. 3(a), is blocked, i.e., it is transformed into an immobile or blocked TD, shown with an “x” in Fig. 3(a). The differential motion $d\lambda$ of the mobile TDs will also lead to probability of reactions between mobile TDs. If we assume that the mobile TDs will react if they fall within an annihilation radius r_A , then the motion $\Delta\lambda$ of the mobile TD sweeps out an interaction area $S = 2r_A\Delta\lambda$, as shown in a schematic plan view in Fig. 3(b). In the area S , each mobile TD on average will encounter $N^m = \rho_{TD}^m S$ other mobile TDs and thus $\Delta\rho_{TD}^m = -N^m\rho_{TD}^m = -\rho_{TD}^m S = -2r_A\rho_{TD}^m\Delta\lambda$. Taking the limit that $\Delta\lambda$ becomes vanishingly small leads to the differential expression $d\rho_{TD}^m = -2r_A\rho_{TD}^m d\lambda$. The mobile TDs may also come within r_A of blocked TDs and annihilate. In the motion $\Delta\lambda$ of the mobile TD, each mobile TD will on average encounter $N^i = \rho_{TD}^i S$ immobile TDs. The differential change in the density of mobile TDs as a result of annihilation reactions with immobile TDs will then be $d\rho_{TD}^m = -2r_A\rho_{TD}^m\rho_{TD}^i d\lambda$. The sum of the three contributions that lead to changing ρ_{TD}^m is then written as

$$d\rho_{TD}^m = -\rho_{TD}^m\rho_{MD}d\lambda - 2r_A\rho_{TD}^m d\lambda - 2r_A\rho_{TD}^m\rho_{TD}^i d\lambda. \quad (7)$$

Immobile TDs are generated by MDs blocking the motion of mobile TDs, i.e., $d\rho_{TD}^i = +\rho_{TD}^i\rho_{MD}d\lambda$, and eliminated by annihilation with mobile TDs, i.e., $d\rho_{TD}^i = -2r_A\rho_{TD}^m\rho_{TD}^i d\lambda$. Thus, the total change in ρ_{TD}^i with motion is given as

$$d\rho_{TD}^i = +\rho_{TD}^i\rho_{MD}d\lambda - 2r_A\rho_{TD}^m\rho_{TD}^i d\lambda. \quad (8)$$

The MDs are generated through the motion of mobile TDs, and their density changes with differential motion as

$$d\rho_{MD} = \frac{1}{2}\rho_{TD}^m d\lambda, \quad (9)$$

where the factor of $\frac{1}{2}$ accounts for use of a linear MD density in a cross-grid array of MDs.

When the misfit strain has been relieved to its equilibrium value for the given film thickness [when ϵ_x given by Eq. (5) is zero], then we consider no further MD generation. In the models developed below, we will investigate the TD reduction and MD generation both at constant film thickness (allowing the system to evolve towards equilibrium) and at changing film thickness (associated with growth). For the TD reactions, we will only consider TD–TD reactions due to TD motion associated with MD generation—unlike our models for homogeneous buffer layers, we will not consider any geometrical motion of the TDs with changing film thickness that is associated with their line direction.

We will develop two main models for TD reduction in strained layers. The first model intentionally neglects blocking of TD motion by other MDs (case I). Although this model may have limited applicability to discretely strained layers, we believe that this model represents the case of graded layers. The second model explicitly treats blocking of TDs by MDs (case II). For both models, we consider cases in

which the mobile TD velocity is constant (until equilibrium relaxation is achieved) or the mobile TD velocity is proportional to the “excess strain” in the system.

For the purposes of compactness, we introduce the notation

$$\begin{aligned} \rho_{TD}^m &= \rho_1, \\ \rho_{TD}^i &= \rho_2, \\ \rho_{MD} &= \rho_3, \end{aligned} \quad (10)$$

and thus Eq. (6) can be rewritten as

$$\rho_{TD}^{\text{total}} = \rho_t = \rho_1 + \rho_2. \quad (11)$$

Additionally, we will frequently use dimensionless TD and MD densities, film thickness, critical thickness, and Burgers vector as a result of normalization by either the annihilation radius squared or by the annihilation radius r_A , respectively, i.e.,

$$\begin{aligned} \tilde{\rho}_1 &= \rho_1 r_A^2 = \rho_{TD}^m r_A^2, \\ \tilde{\rho}_2 &= \rho_2 r_A^2 = \rho_{TD}^i r_A^2, \\ \tilde{\rho}_3 &= \rho_3 r_A = \rho_{MD} r_A, \\ \tilde{h} &= \frac{h}{r_A}, \\ \tilde{h}_c &= \frac{h_c}{r_A}, \\ \tilde{b} &= \frac{b}{r_A}, \\ \tilde{\lambda} &= \frac{\lambda}{r_A}. \end{aligned} \quad (12)$$

We prefer to work with both the dimensional form and the normalized form (dimensionless) of the coupled differential equations and variables. The dimensional form is included here for the sake of the derivation. The normalized variables and equations are used because they reduce the number of independent parameters and the results have broader applicability.

A. General form of the differential equations

Using the compact notation for the TD and MD densities given above, the coupled differential equations describing the TD and MD evolution are given as

$$d\rho_1 = -q\rho_1\rho_3 d\lambda - 2r_A\rho_1^2 d\lambda - 2qr_A\rho_1\rho_2 d\lambda, \quad (13a)$$

$$d\rho_2 = q(\rho_1\rho_3 d\lambda - 2r_A\rho_1\rho_2 d\lambda), \quad (13b)$$

$$d\rho_3 = \frac{1}{2}\rho_1 d\lambda, \quad (13c)$$

where the parameter q represents MDs blocking or not blocking TD motion ($q=1$ corresponds to blocking of TDs by MDs and $q=0$ corresponds to no blocking). The coupled differential equations written in normalized form are given as

$$d\tilde{\rho}_1 = -q\tilde{\rho}_1\tilde{\rho}_3 d\tilde{\lambda} - 2\tilde{\rho}_1^2 d\tilde{\lambda} - 2q\tilde{\rho}_1\tilde{\rho}_2 d\tilde{\lambda}, \quad (14a)$$

$$d\tilde{\rho}_2 = q(\tilde{\rho}_1\tilde{\rho}_3d\tilde{\lambda} - 2\tilde{\rho}_1\tilde{\rho}_2d\tilde{\lambda}), \quad (14b)$$

$$d\tilde{\rho}_3 = \frac{1}{2}\tilde{\rho}_1d\tilde{\lambda}. \quad (14c)$$

The motion of the mobile TDs is limited either by realization of complete strain relaxation ($\rho_3b = \epsilon_m$), when there is no driving force for continued motion, or through their depletion by annihilation reactions and the formation of blocked TDs. Since λ is not an easily controlled experimental parameter (nor is it easily measured), in several cases we relate the TD motion to easily realized parameters such as film thickness or growth rate.

IV. SPECIFIC CASES

We now consider several solutions to the set of coupled differential equations [Eqs. (13) or (14)] for different boundary conditions. Although the solutions are general, we will consider examples for which the magnitude of the Burgers vector is $\sim 1\text{--}5 \text{ \AA}$, which is in the typical range for group IV and zinc blende semiconductors, the misfit strain ϵ_m is in the range $10^{-4}\text{--}10^{-1}$ (although this latter value is very large, it could be easily realized in graded layer growth), and the annihilation radius r_A has a value in the range $500\text{--}1000 \text{ \AA}$.⁴

A. Case I.1: No blocking, equilibrium relaxation

In this case, we neglect any blocking of TD motion by MD segments that lie at the strained layer/substrate interface. In this model equilibrium relaxation is achieved [see Eq. (4)] and all TDs are assumed to generate MD segments starting at $h = h_c$. Thus, the TD motion $d\lambda$ with changing film thickness dh may be determined by

$$\rho_3 = \frac{1}{h_c} - \frac{1}{h}, \quad (15a)$$

$$d\rho_3 = \frac{dh}{h^2} = \frac{1}{2}\rho_1d\lambda, \quad (15b)$$

which gives

$$d\lambda = \frac{2dh}{\rho_1h^2} = \frac{2\epsilon_m h_c dh}{b\rho_1h^2}, \quad (16)$$

where we have used $h_c = b/\epsilon_m$. Since there is no blocking, $\rho_2 = 0$ for all film thicknesses [i.e., $q = 0$ in Eqs. (13) or (14)], this reduces the system [Eqs. (13) or (14)] to two independent differential equations:

$$d\rho_1 = -\frac{4r_A\epsilon_m}{b} \frac{h_c}{h^2} \rho_1 dh, \quad (17a)$$

$$d\rho_3 = \frac{\epsilon_m}{b} \frac{h_c}{h^2} dh. \quad (17b)$$

These two equations can be integrated from h_c to $h(>h_c)$ using the boundary conditions

$$\rho_1|_{h=h_c} = \rho_1^0$$

and

$$\rho_3|_{h=h_c} = 0$$

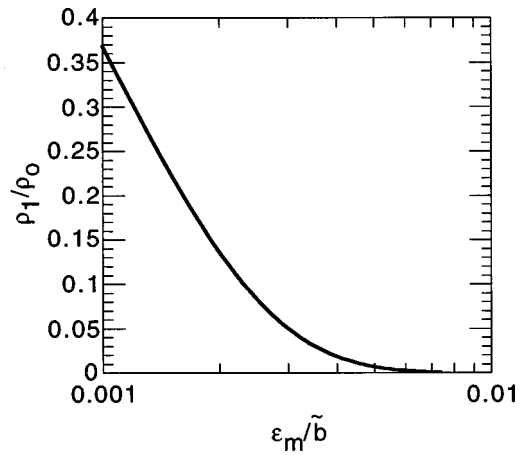


FIG. 4. TD reduction, ρ_1/ρ_1^0 , in the model of no TD blocking for fully relaxed layers ($h \rightarrow \infty$) as a function of the initial misfit strain ϵ_m divided by the normalized Burgers vector $\epsilon_m/\tilde{b} = \epsilon_m r_A/b [= (r_A/h_c)]$.

to give

$$\rho_1 = \rho_1^0 \exp\left[-B\left(1 - \frac{h_c}{h}\right)\right], \quad (18a)$$

$$\rho_3 = \frac{\epsilon_m}{b} \left(1 - \frac{h_c}{h}\right), \quad (18b)$$

where $B = 4r_A\epsilon_m/b = 4\epsilon_m/\tilde{b}$. We note that it is obvious that Eq. (18b) is just another form of Eq. (15a). For $h = h_c$, there is no strain relaxation or TD reduction, as anticipated. For $h \rightarrow \infty$,

$$\rho_1 = \rho_1^0 \exp(-B), \quad (19a)$$

$$\rho_3 = \frac{\epsilon_m}{b} = \rho_3^\infty, \quad (19b)$$

where ρ_3^∞ corresponds to the MD density for the fully relaxed layer.

Assuming that there is no blocking of TDs by MDs or by other TDs this solution predicts a decrease in TD density that depends exponentially on the parameter B . The misfit strain is the most directly controlled parameter in B , and small changes in the misfit strain can lead to substantial changes in the final TD density. As a simple estimate, we take $b = 2 \text{ \AA}$, $r_A = 500 \text{ \AA}$ and plot $\rho_1^{\text{final}}/\rho_1^0$ as a function of the nominal misfit strain for the layer in Fig. 4. It can be seen that a misfit strain of 0.1% leads to a $\sim 66\%$ TD reduction of and a 1% misfit strain leads to a TD reduction of $\sim 99.5\%$.

Although this model shows that substantial TD reduction can be achieved by a single strained layer, it is unlikely that such reduction would be realized because of blocking of TD motion by MDs. However, for the case of strain graded layers, in which the MDs are distributed throughout the strained region, this model may have more applicability; this is because the strain grading provides a means for TDs to bypass other MDs.

B. Case I.2: No blocking, equilibrium relaxation, and diminishing driving force

In this model, we assume that the TD velocities are linearly proportional to the “excess strain” for relaxation [see Eq. (5)] and we relate the differential TD motion to both the TD velocity and to the film growth rate. Again in this model, we consider no obstacles to TD motion (i.e., no blocking of TDs by MDs).

The TD velocity is taken as linearly proportional to the excess strain in the system. The functional dependence for the velocity does not change the asymptotic value of the TD densities provided that the TDs have zero velocity for $\epsilon_x = 0$. The average TD velocity v will be given as

$$v = A \epsilon_x = A \left[\epsilon_m \left(1 - \frac{h_c}{h} \right) - \rho_3 b \right] = A \left[\epsilon_m \left(1 - \frac{\tilde{h}_c}{\tilde{h}} \right) - \tilde{\rho}_3 \tilde{b} \right], \quad (20)$$

where A is a proportionality constant with units length/time. The differential TD motion $d\lambda$ will be $d\lambda = v dt$. For constant film growth rate, $g = dh/dt$, $d\lambda = v dt = (v/g)dh$, and thus the coupled differential equations for TD and MD density evolution can be written as

$$d\rho_1 = -2r_A \rho_1^2 a \left[\epsilon_m \left(1 - \frac{h_c}{h} \right) - \rho_3 b \right] dh, \quad (21a)$$

$$d\rho_3 = \frac{1}{2} \rho_1 a \left[\epsilon_m \left(1 - \frac{h_c}{h} \right) - \rho_3 b \right] dh, \quad (21b)$$

or in dimensionless form

$$d\tilde{\rho}_1 = -2\tilde{\rho}_1^2 a \left[\epsilon_m \left(1 - \frac{\tilde{h}_c}{\tilde{h}} \right) - \tilde{\rho}_3 \tilde{b} \right] d\tilde{h}, \quad (22a)$$

$$d\tilde{\rho}_3 = \frac{1}{2} \tilde{\rho}_1 a \left[\epsilon_m \left(1 - \frac{\tilde{h}_c}{\tilde{h}} \right) - \tilde{\rho}_3 \tilde{b} \right] d\tilde{h}, \quad (22b)$$

where $a = A/g$. This system of equations can be solved numerically since they are coupled through the variable ρ_1 .

Since this model does not include TD blocking, the solutions should asymptotically approach the solutions for TD and MD density given at large film thicknesses, as given in Eqs. (19). The rate of TD density falloff should decrease with decreasing a values. Figure 5 shows the solutions to Eqs. (22) for $\epsilon_m = 0.01$, $b = 10^{-2} r_A$, $\rho_1^0 r_A^2 = 0.2$, and for a values of 10, 100, and 1000 (if we take, for example, $r_A = 500 \text{ \AA}$, then $b = 5 \text{ \AA}$ and $\rho_1^0 = 8 \times 10^9 \text{ cm}^{-2}$). These solutions show that the TD density does fall with increasing film thickness and asymptotically approaches its saturation value at large \tilde{h} . Furthermore, the TD density has a faster rate of diminishment for increasing TD velocity. Figure 5 also shows the calculated TD density for the case of equilibrium relaxation [case I.1, Eq. (18a)]. In all cases where the TD velocity depends on the excess strain, the TD density has a higher value than that given by the case of equilibrium relaxation. This is the expected result, because equilibrium relaxation corresponds to zero excess strain ϵ_x throughout the growth.

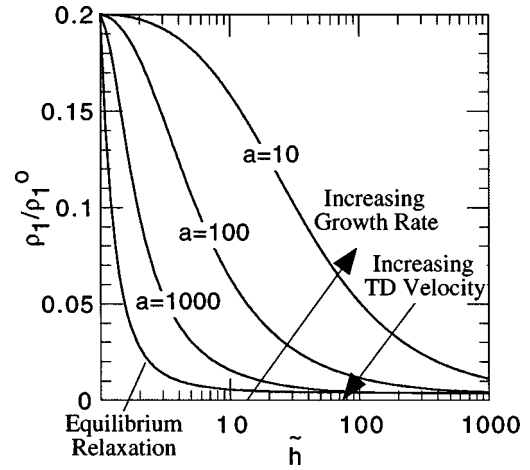


FIG. 5. Thickness dependence of the TD density in strained layers in the model without blocking where the TD velocity is proportional to the “excess” strain (case I.2). Curves are shown for different a values (where a is proportional to the ratio of the TD velocity to growth rate). Additionally, the solution is shown for equilibrium relaxation [see Eq. (18a)]. The initial misfit strain here is $\epsilon_m = 0.01$.

C. Case II.1: Blocking, no annihilation reactions (constant driving force)

In this case, we consider only blocking of mobile TDs by MDs, thus creating blocked TDs; there is no annihilation of TDs. For this idealized situation, the following three equations must be solved:

$$d\rho_1 = -\rho_1 \rho_3 d\lambda, \quad (23a)$$

$$d\rho_2 = \rho_1 \rho_3 d\lambda, \quad (23b)$$

$$d\rho_3 = \frac{1}{2} \rho_1 d\lambda. \quad (23c)$$

For these equations, it is obvious that $d\rho_2 = -d\rho_1$ and direct integration gives $\rho_2 = -\rho_1 + C$ (C is an integration constant). Thus only two coupled equations must be solved:

$$\frac{d\rho_1}{d\lambda} = -\rho_1 \rho_3, \quad (24a)$$

$$\frac{d\rho_3}{d\lambda} = \frac{1}{2} \rho_1, \quad (24b)$$

where

$$\lambda|_{h=h_c} = 0, \quad \rho_1|_{h=h_c} = \rho_1^0, \quad \rho_2|_{h=h_c} = 0,$$

and

$$\rho_3|_{h=h_c} = 0,$$

which leads to $C = \rho_1^0$. The solution of these equations is given as

$$\rho_1 = \frac{4\rho_1^0 \exp(\sqrt{\rho_1^0} \lambda)}{[\exp(\sqrt{\rho_1^0} \lambda) + 1]^2}, \quad (25a)$$

$$\rho_3 = \sqrt{\rho_1^0} \frac{\exp(\sqrt{\rho_1^0} \lambda) - 1}{\exp(\sqrt{\rho_1^0} \lambda) + 1}, \quad (25b)$$

which have the asymptotic behavior:

$$\lim_{\lambda \rightarrow \infty} \rho_1 = 0, \quad (26a)$$

$$\lim_{\lambda \rightarrow \infty} \rho_3 = \sqrt{\rho_1^0}. \quad (26b)$$

Although these solutions neglect TD annihilation, they do demonstrate the general validity of the approach. Provided that there is sufficient misfit strain, all mobile TDs will become blocked by MDs. Since each mobile TD generates a MD segment in this model, the final MD density is given as the square root of the TD density and the maximum strain relaxation is given as $\rho_3 b = \sqrt{\rho_1^0} b$. Taking, for example, $\rho_1^0 = 10^{10} \text{ cm}^{-2}$ and $b = 2 \text{ \AA}$, the maximum strain relaxation is $\rho_3 b = \sqrt{\rho_1^0} b = 2 \times 10^{-3}$. It is important to note that when annihilation and blocking reactions are included (see the next case) the plastic strain relaxation, $\rho_3 b$, will be less than that predicted by Eq. (26b) because the density of mobile TDs is diminishing through annihilation, thus reducing the density of TDs that can produce new MD segments.

Let us consider strain layer growth on high quality single crystal substrates, e.g., GaAs with a TD density of $\sim 10^4 \text{ cm}^{-2}$, and an effective value of b of $\sim 2 \text{ \AA}$. The maximum extent of strain relaxation from MDs that result from bending of substrate TD in the blocking limit will be $\rho_3 b = \sqrt{\rho_1^0} b = 2 \times 10^{-6}$. Thus, it is not surprising that the new TDs must be generated for extensive relaxation in strained layer growth on high quality substrates.

D. Case II.2: Blocking, reactions, incomplete relaxation (diminishing driving force)

This case involves solutions of Eqs. (13) (with $q=1$) corresponding to both TD annihilation reactions and blocking of mobile TDs by MDs. In this case, the TD velocity is linearly proportional to the ‘‘excess’’ strain in the system of differential equations which readily facilitates solutions in thickness, an experimental parameter, rather than λ . Although the TD velocity likely has a power law or exponential dependence on the excess strain, the TD and MD densities for large thicknesses (asymptotic values) will not change. The equations to be solved follow as

$$d\rho_1 = -a \left[\epsilon_m \left(1 - \frac{h_c}{h} \right) - \rho_3 b \right] (\rho_1 \rho_3 + 2r_A \rho_1^2 + 2r_A \rho_1 \rho_2) dh, \quad (27a)$$

$$d\rho_2 = a \left[\epsilon_m \left(1 - \frac{h_c}{h} \right) - \rho_3 b \right] (\rho_1 \rho_3 - 2r_A \rho_1 \rho_2) dh, \quad (27b)$$

$$d\rho_3 = \frac{a}{2} \left[\epsilon_m \left(1 - \frac{h_c}{h} \right) - \rho_3 b \right] \rho_1 dh, \quad (27c)$$

or in normalized form as

$$\frac{d\tilde{\rho}_1}{d\tilde{h}} = -a\tilde{b} \left(\frac{1}{\tilde{h}_c} - \frac{1}{\tilde{h}} - \tilde{\rho}_3 \right) (\tilde{\rho}_1 \tilde{\rho}_3 + 2\tilde{\rho}_1^2 + 2\tilde{\rho}_1 \tilde{\rho}_2), \quad (28a)$$

$$\frac{d\tilde{\rho}_2}{d\tilde{h}} = a\tilde{b} \left(\frac{1}{\tilde{h}_c} - \frac{1}{\tilde{h}} - \tilde{\rho}_3 \right) (\tilde{\rho}_1 \tilde{\rho}_3 - 2\tilde{\rho}_1 \tilde{\rho}_2), \quad (28b)$$

$$\frac{d\tilde{\rho}_3}{d\tilde{h}} = \frac{a\tilde{b}}{2} \left(\frac{1}{\tilde{h}_c} - \frac{1}{\tilde{h}} - \tilde{\rho}_3 \right) \tilde{\rho}_1. \quad (28c)$$

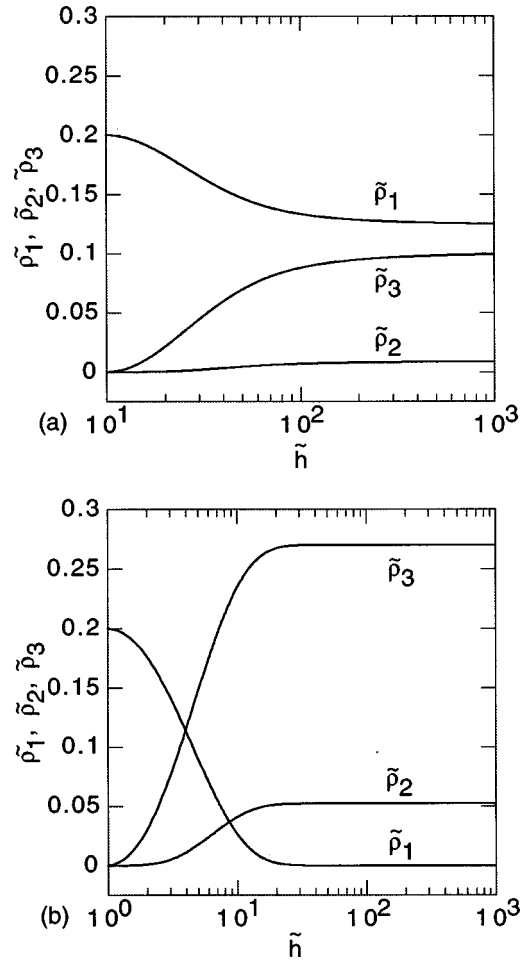


FIG. 6. Evolution of TD and MD densities in growing strained layers [examples of solutions of the system of Eqs. (28)] in the model that includes TD blocking by MDs and TD velocity proportional to the ‘‘excess’’ strain. (a) Growth with complete misfit strain relaxation; (b) growth with incomplete misfit strain relaxation. For (a) and (b) the following parameters were used: normalized initial TD density $\tilde{\rho}_1^0 = \rho_1^0 / r_A^2 = 0.2$; $a = 100$ (TD velocity parameter); and normalized Burgers vector $\tilde{b} = b / r_A = 0.01$. The initial misfit strain for (a) was $\epsilon_m = 0.001$ and for (b) $\epsilon_m = 0.01$.

We start by considering two representative examples of the solutions of Eqs. (28) in which either the misfit strain is completely relaxed or all mobile TDs become blocked before the strain can be fully relaxed. For this example, $b = 10^{-2} r_A$, $\rho_1^0 r_A^2 = 0.2$, $a = 100$, and $\epsilon_m = 0.001$ [Fig. 6(a)] or $\epsilon_m = 0.01$ [Fig. 6(b)]. For the case of the initial misfit $\epsilon_m = 0.001$, the normalized MD density $\tilde{\rho}_3$ asymptotically approaches a value of 0.1 for large \tilde{h} which corresponds to complete strain relaxation [$(\tilde{\rho}_3 / r_A) b = \rho_3 b = (0.1 / r_A) 10^{-2} \times r_A = 10^{-3}$]. For this example, the normalized density of mobile TDs $\tilde{\rho}_1$ and blocked TDs $\tilde{\rho}_2$ both asymptotically approach a constant value with increasing \tilde{h} , as expected for complete strain relaxation; as the film relaxes, there is a diminishing driving force for TD motion and new MD formation. Since the misfit strain is small, the TD reduction is also small, $\tilde{\rho}_1^{\text{final}} / \tilde{\rho}_1^0 \approx 0.65$. If there were no blocking (and in this case there is minimal blocking as $\tilde{\rho}_2^{\text{final}} / \tilde{\rho}_1^{\text{final}} < 0.1$), then, using Eq. (19a), a fraction change in TD density $\tilde{\rho}_1^{\text{final}} / \tilde{\rho}_1^0 = 0.670$ is predicted which is in close agreement with the numerical solution.

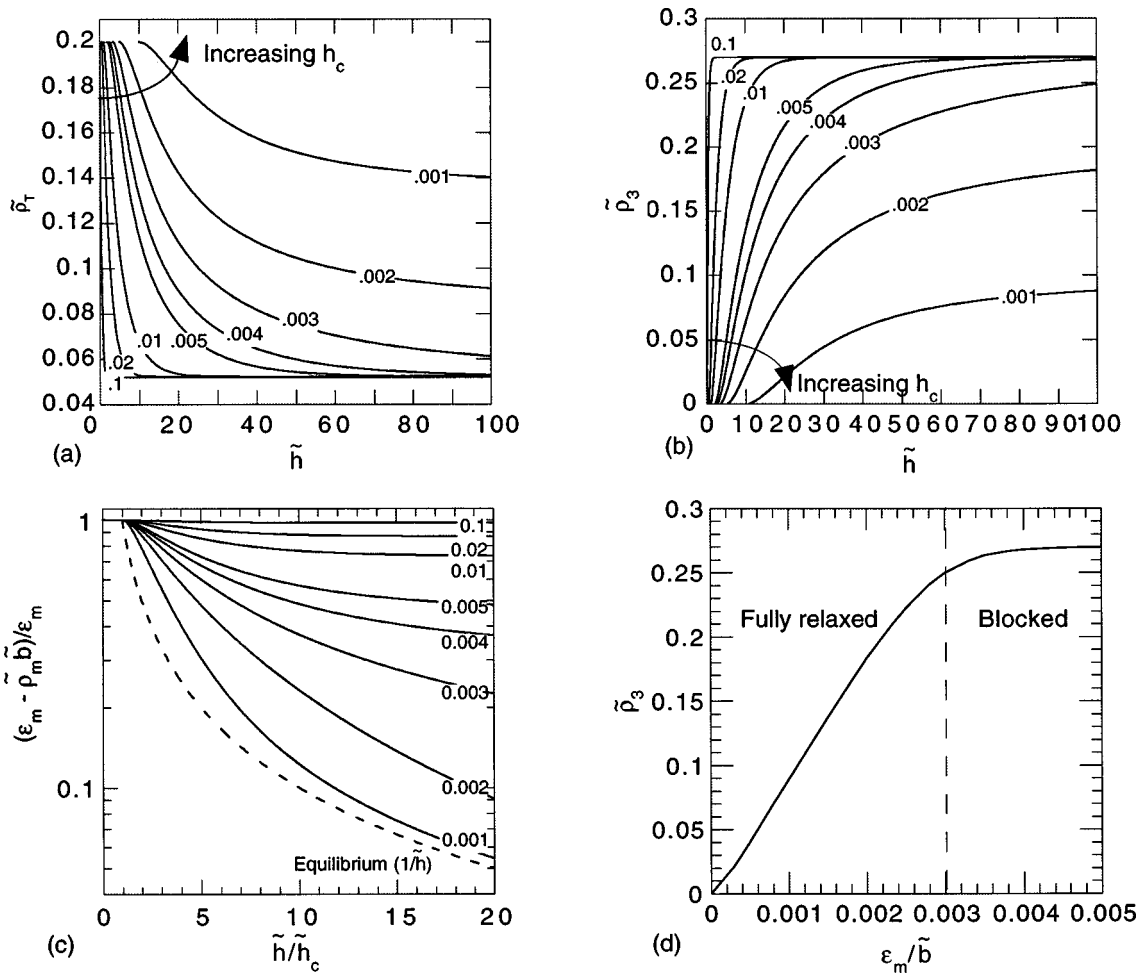


FIG. 7. Solutions of the system of Eqs. (27) or (28) corresponding to the model that includes TD blocking by MDs and TD velocity proportional to the "excess" strain. These plots show the thickness dependence of the total TD density and MD density in strained layers for different initial misfit strain ϵ_m . (a) Total normalized TD density $\tilde{\rho}_t = \tilde{\rho}_1 + \tilde{\rho}_2 (= \rho_1 r_A^2 = \rho_1 r_A^2 + \rho_2 r_A^2)$; (b) normalized MD density $\tilde{\rho}_3 = \rho_3 r_A$; (c) fractional residual strain $(\epsilon_m - \tilde{\rho}_3 \tilde{b})/\epsilon_m = (\epsilon_m - \rho_3 b)/\epsilon_m$. The initial misfit strains $\epsilon_m = 0.001, 0.002, 0.003, 0.004, 0.005, 0.01, 0.02$, and 0.1 are shown for each curve. For all parts the following parameters were used: $\tilde{\rho}_1^0 = \rho_1^0 r_A^2 = 0.2$; $a = 100$ (TD velocity parameter); and $\tilde{b} = b/r_A = 0.01$. The dashed line in (c) corresponds to the equilibrium residual strain, which can be found from Eq. (3). (d) Dependence of the normalized MD density $\tilde{\rho}_3 = \rho_3 r_A$ on the normalized initial misfit strain $\epsilon_m/\tilde{b} = \epsilon_m r_A/b$.

When the strain is sufficiently large, the TDs will become blocked before the film fully relaxes, as shown in Fig. 6(b) for the case where $\epsilon_m = 0.01$. In this example, the normalized MD density $\tilde{\rho}_3$ asymptotically approaches a value of ~ 0.27 for large \tilde{h} which corresponds to a plastic strain of 2.7×10^{-3} . For complete blocking, the final value of $\tilde{\rho}_3$ can be compared with the asymptotic behavior of Eqs. (26) which are the solutions for the TD evolution when annihilation is neglected. In this case, $\max_{\rho_1 \rightarrow 0} \tilde{\rho}_3 = \sqrt{\tilde{\rho}_1^0} = 0.447$. The asymptotic value of $\tilde{\rho}_3$ is less than $\sqrt{\tilde{\rho}_1^0}$ because the value of $\tilde{\rho}_1$ decreases through annihilation reactions in addition to blocking reactions.

The solutions to Eqs. (28) are quite stable when the system either approaches complete relaxation [Fig. 6(a)] or exhausts itself of mobile TDs [Fig. 6(b)]. Solutions for Eqs. (28) for different velocity dependence on strain (i.e., cases where the TD velocity has a power law dependence on the excess strain; $v = A \epsilon_x^n$) have the same asymptotic values of the TD and MD densities.

For the case of complete relaxation, the extent of the

total TD reduction (where $\rho_{TD}^{total} = \rho_t = \rho_1 + \rho_2$ or $\tilde{\rho}_{TD}^{total} = \tilde{\rho}_t = \tilde{\rho}_1 + \tilde{\rho}_2$) increases with increasing misfit strain. However, when the misfit strain exceeds the value where complete relaxation is possible (referred to as the blocking limit, i.e., $\tilde{\rho}_1 \rightarrow 0$ for increasing \tilde{h}), the change in total TD density is constant for the same initial TD density. Figure 7(a) shows the thickness dependence of $\tilde{\rho}_t$ for different values of ϵ_m ranging between 0.001 and 0.1 for an initial TD density $\tilde{\rho}_1^0 = 0.2$. For misfit strains larger than ~ 0.003 , the total TD density asymptotically approaches a value of ~ 0.055 , corresponding to a TD reduction of $\sim 75\%$. The MD density $\tilde{\rho}_3$ also reaches a constant value for misfit strains larger than ~ 0.003 , as shown in Fig. 7(b). The value of the normalized residual strain $(\epsilon_m - \tilde{\rho}_3 \tilde{b})/\epsilon_m = (\epsilon_m - \rho_3 b)/\epsilon_m$ as a function of thickness is shown in Fig. 7(c). Again, it is clear that for initial misfit strains less than ~ 0.003 there are sufficient mobile TDs to eventually fully relax the misfit strain, whereas for initial misfit strains greater than ~ 0.003 , the mobile TDs become exhausted and the films have a residual misfit strain.

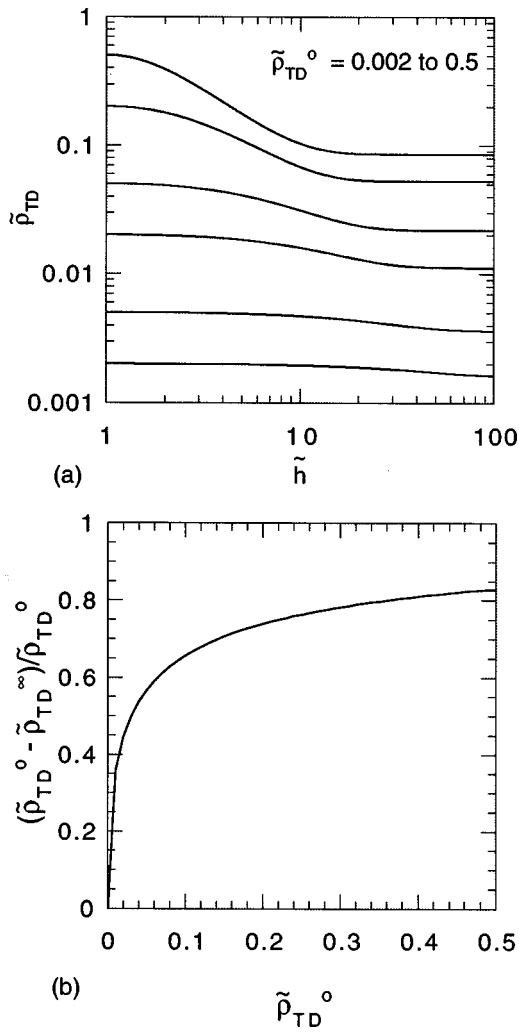


FIG. 8. Influence of the initial value of the TD density on the relaxation processes in strained epitaxial layers (for the model that includes blocking and a linear dislocation velocity dependence on the “excess” strain). (a) Evolution of the normalized TD density $\tilde{\rho}_i = \tilde{\rho}_1 + \tilde{\rho}_2 (= \rho_i r_A^2 = \rho_1 r_A^2 + \rho_2 r_A^2)$ with normalized film thickness $\tilde{h} = h/r_A$. (b) Dependence of the maximum possible TD reduction $(\tilde{\rho}_i^0 - \tilde{\rho}_i^\infty)/\tilde{\rho}_i^0 = (\rho_i^0 - \rho_i^\infty)/\rho_i^0$ in the blocking model as a function of the normalized initial TD density $\tilde{\rho}_i^0 = \rho_i^0 r_A^2$. Here, the following parameters were used: initial misfit $\epsilon_m = 0.01$ and $a = 100$ (TD velocity parameter).

The asymptotic values of the misfit dislocation density $\tilde{\rho}_3$ as a function of the initial misfit strain are shown in Fig. 7(d).

The fractional TD reduction, in the model including blocking and diminishing driving force with progressive strain relaxation, depends explicitly on the number of initial TDs. This is shown in Figs. 8(a) and 8(b). In these examples, the initial misfit strain is 0.01, $h_c = r_A$, and a velocity parameter $a = 100$ was used. For small initial TD density, there is negligible reduction, as the TDs have large spacing relative to r_A and there is only a small probability of reaction of either two mobile TDs or one mobile TD and one blocked TD. With increasing TD density, the probability of reaction increases, and there is a more effective percentage reduction, as shown in Fig. 8 (b).

V. DISCUSSION

The use of discretely strained layers can provide a marked reduction in TD density, as shown in the models

developed in this article. Discretely strained layers are particularly effective at TD reduction for initially high TD densities. However, at lower initial TD densities, the probability of TD–TD reactions is diminished through the blocking of mobile TDs by MDs. When there is sufficient “excess” strain, blocked TDs may by pass the MD segment which lies in the TD glide path; however, adoption of a “bypass criterion” has not been included in our initial approach but is planned for future work.

Alternative approaches to TD reduction, such as continuously graded layers, may be employed for effective TD reduction at lower TD densities or for achieving over all lower TD densities. Provided that the strain grading is sufficiently slow with increasing film thickness, graded layers provide the intrinsic advantage that the MDs are distributed throughout the strained layer and thus blocking of mobile TDs by MD segments is avoided (for reviews for experimental results on graded layers, see either Ref. 1 or 14). Thus, the model of no blocking of mobile TDs and equilibrium relaxation (case I.1) should represent the ideal limit for slowly graded layers; the total TD density should have an exponential dependence on the annihilation radius and on the total misfit strain. Further, for a slowly graded layer, the product of the projected misfit dislocation density $\rho_3^{\text{projected}}$ (projected through the fully graded layer) and the Burgers vector should be equal to the total misfit strain for the graded layer, i.e., $\rho_3^{\text{projected}} b = \epsilon_m$. Recent results indicate that graded layer approaches have had the most success in reducing TD densities for laterally uniform layers (for example, see two recent articles, Refs. 15 and 16).

In this work, we have assumed that during the growth of the strained layer there is insufficient driving force to activate new sources of misfit and threading dislocations. However, in the growth of strained layers, either where the TD density is low (such as in the growth on high quality substrates) or where either the misfit strain or thickness is large, then the possibility of activating sources for new MDs and TDs may be quite high.¹⁷ The current treatment has explicitly been concerned with reducing TD density through strain-driven motion of TDs. For real growths, however, the possibility of increasing the TD density through the activation of new dislocation sources is a real issue that requires careful experimental consideration. In our future work, we will explicitly deal with possible dislocation generation.

In our previous modeling of TD evolution in relaxed homogeneous buffer layers, we suggested that fluctuations of the net Burgers content of the TDs may give rise to saturation of the final TD density, where the important fluctuation wavelength is on the order of or larger than the possible lateral motion of the TDs. For the case of homogeneous buffer layers, the extent of lateral TD motion is determined by the trajectory of the inclined TD with increasing film thickness. However, for strained layers, the extent of lateral TD motion depends on the nominal misfit strain and the initial total TD density. In principal, the lateral TD motion for strained layers may be substantially larger than the lateral motion achievable for homogeneous buffer layers. Therefore, the strain-driven migration of the TDs may act to “homogenize” the spatial distribution of densities of different

specific TDs and thus lead to a lower value of the local net Burgers vector content and, accordingly, lower saturation values of the TD density. Indeed, MacPherson and Goodhew showed that the growth of strained $\text{In}_{0.10}\text{Ga}_{0.90}\text{As}$ layers on GaAs substrates with a thickness $h \approx 4h_c$ leads to both an order of magnitude reduction in TD density and also leads to reduced inhomogeneities in the distribution of threading dislocations.¹⁸

VI. SUMMARY AND CONCLUSIONS

In this article, we have developed models for TD reduction due to the introduction of an intentionally strained layer. Since this effort has been focused on TD reduction, we have not included mechanisms that would increase the TD density (i.e., we have not accounted for any multiplication or other generation processes). Three different types of dislocations have been considered in this model: mobile TDs, immobile TDs, and MDs. The models are based on MD formation by the process of lateral TD motion and subsequent annihilation reactions of mobile TDs with either other mobile TDs or blocked TDs, or reactions in which a mobile TD is converted to an immobile TD by a blocking reaction with a MD. The evolution of the density of mobile and blocked TDs and MDs can be represented by three coupled nonlinear first order differential equations.

The two cases in which we have an analytical solution to the coupled differential equations for TD density provide important limits for TD behavior in strained thin films. The case where TD blocking by MD is not considered (case I.1), which may be directly applicable to slowly graded layers, gives the maximum TD reduction for a total misfit strain ϵ_m , regardless whether the layer is discretely strained, step-graded, or continuously graded. The ratio of the final to initial TD density depends exponentially on the annihilation radius r_A and on the total misfit strain ϵ_m [see Eq. (19a)].

The case where only blocking reactions were considered (case II.1) provides the upper limit for plastic strain relaxation for a discretely strained layer. The maximum possible strain relaxation is simply given as $\rho_3 b = \sqrt{\rho_1^0} b$. Once a layer has approached the maximum possible strain relaxation given by the blocking limit (nearly complete diminishment of mobile TDs), further increases in the layer thickness may lead to the activation of new sources of TDs and MDs. This result has significance in the design of discretely strained layers or step-graded layers for TD reduction. This result shows that in step-graded layers for TD reduction the misfit strain between subsequent steps should have *decreasing*

magnitude and the subsequent steps should have *increasing* thickness to allow for sufficient relaxation of the reduced layer thickness.

Numerical solutions for the cases that include both annihilation and blocking reactions have behavior bounded by the two analytic cases. The solution to these equations, when the TD velocity is proportional to the excess strain, show stable solutions, thus demonstrating the general validity of the approach.

ACKNOWLEDGMENTS

This work was supported in part by the U.S. Air Force Office of Scientific Research through the PRET center at the University of California, Santa Barbara (Dr. Gerald Witt contract monitor). Travel support for two of the authors (J.S.S. and W.P.) was provided by the travel program of the NSF under Award No. INT-9603242. One author (A.E.R.) was supported in part by the Russian Research Council program, Physics of Solid Nanostructures, Project No. 97-3006 and SFB Project No. 422 of DFG (Germany).

¹R. Beanland, D. J. Dunstan, and P. J. Goodhew, *Adv. Phys.* **45**, 87 (1996).

²L. B. Freund, *Mater. Res. Bull.* **17**, 52 (1992).

³E. A. Fitzgerald, *Mater. Sci. Rep.* **7**, 87 (1991).

⁴J. S. Speck, M. A. Brewer, G. E. Beltz, A. E. Romanov, and W. Pompe, *J. Appl. Phys.* **80**, 3808 (1996).

⁵A. E. Romanov, W. Pompe, G. E. Beltz, and J. S. Speck, *Appl. Phys. Lett.* **69**, 3342 (1996).

⁶A. E. Romanov, W. Pompe, G. Beltz, and J. S. Speck, *Phys. Status Solidi B* **198**, 599 (1996).

⁷A. E. Romanov, W. Pompe, G. Beltz, and J. S. Speck, *Phys. Status Solidi B* **199**, 33 (1997).

⁸G. E. Beltz, M. Chang, J. S. Speck, A. E. Romanov, and W. Pompe, *Philos. Mag. A* **76**, 807 (1997).

⁹M. Y. Martisov and A. E. Romanov, *Sov. Phys. Solid State* **33**, 1173 (1991).

¹⁰S. J. Barnett, A. M. Keir, A. G. Cullis, A. D. Johnson, J. Jefferson, G. W. Smith, T. Martin, C. R. Whitehouse, G. Lacey, G. F. Clark, B. K. Tanner, W. Spirkl, B. Lunn, J. C. H. Hogg, W. E. Hagston, and C. M. Castelli, *J. Phys. D* **28**, A17 (1995).

¹¹L. B. Freund, *J. Appl. Phys.* **68**, 2073 (1990).

¹²V. T. Gillard, W. D. Nix, and L. B. Freund, *J. Appl. Phys.* **76**, 7280 (1994).

¹³J. Y. Tsao, *Materials Fundamentals of Molecular Beam Epitaxy* (Academic, New York, 1993).

¹⁴P. Kidd, D. J. Dunstan, H. G. Colson, M. A. Lourenco, A. Sacedon, F. Gonzalez-Sanz, L. Gonzalez, Y. Gonzalez, R. Garcia, D. Gonzalez, F. J. Pacheco, and P. J. Goodhew, *J. Cryst. Growth* **169**, 649 (1996).

¹⁵M. T. Currie, S. B. Samavedam, T. A. Langdo, C. W. Leitz, and E. A. Fitzgerald, *Appl. Phys. Lett.* **72**, 1718 (1998).

¹⁶M. T. Bulsara, C. Leitz, and E. A. Fitzgerald, *Appl. Phys. Lett.* **72**, 1608 (1998).

¹⁷R. Beanland, *J. Appl. Phys.* **72**, 4031 (1992).

¹⁸G. MacPherson and P. J. Goodhew, *J. Appl. Phys.* **80**, 6706 (1996).